in the extensive spot patterns from bent crystals and in powder patterns.

Our arguments have indicated that the range of crystal thickness for which single-crystal structure analysis is feasible is not limited to the range of validity of the kinematic theory as defined, for example, by the calculations of Blackman (1939) for perfect crystals. If the crystals are perfect, the use of our first-order approximation not only allows crystal structure analysis to be carried out for crystals of greater thickness but provides a technique for the unambiguous determination of crystal structures which involves, in effect, the determination of the relative phases of reflections from series of diffraction patterns obtained with different crystal thicknesses or accelerating voltages. If the crystals are imperfect, it has been shown that the range of validity of the kinematic theory is extended. For both perfect and imperfect crystals it seems probable that the use of higher-order approximations, involving the effects of Fresnel diffraction within the crystal, may extend the range of thickness still further although making the mathematical treatment of the diffraction observations much more cumbersome and requiring more detailed knowledge of crystal thickness and imperfections.

References

Blackman, M. (1939). *Proc. Roy. Soc.* A, **173**, 68.
Cowley, J. M. (1953). *Acta Cryst.* **6**, 516.
Cowley, J. M. (1957). *Acta Cryst.* **10**, 141.
Cowley, J. M. & Moodie, A. F. (1957). *Acta Cryst.* **10**, 609.
Cowley, J. M. & Moodie, A. F. (1958). *Proc. Phys. Soc.* **71**, 533.
Cowley, J. M. & Moodie, A. F. (1959). *Acta Cryst.* **12**, 353.
Cowley, J. M., Rees, A. L. G. & Spink, J. A. (1951). *Proc. Phys. Soc.* A, **64**, 609.
Glauber, R. & Schomaker, V. (1953). *Phys. Rev.* **89**, 667.
Heidenreich, R. D. (1950). *Phys. Rev.* 77, 271.
Ibers, J. A. & Hoerni, J. A. (1954). *Acta Cryst.* **7**, 405.
Schomaker, V. & Glauber, R. (1952). *Nature, Lond.* **170**, 290.

Acta Cryst. (1959). **12**, 367

The Electron-Optical Imaging of Crystal Lattices

By J. M. Cowley

Division of Chemical Physics, Chemical Research Laboratories, Commonwealth Scientific and Industrial Research Organization, Melbourne, Australia

(*Received* 7 *July* 1958)

The theory of the scattering of electrons by crystals previously developed (Cowley & Moodie, 1957*a*) is applied to determine the nature of the image of a crystal lattice obtained with an ideal electron microscope, both in- and out-of-focus. For very thin crystals the pseudo-kinematic theory is applied, and for thick crystals the dynamic theory in a two-beam approximation is used. Intensity anomalies and 'stepped' structures in micrographs showing the 90 Å superlattice spacing of a form of antigorite are explained as arising from simultaneous dynamic scattering of a fundamental lattice reflection and kinematic scattering of the superlattice reflection.

It is shown that dynamic scattering can give rise to variations in the spacing and orientation of moiré-like fringes appearing in electron microscope images of superimposed crystals.

1. Introduction

In recent years a number of observations have been made of periodic intensity modulations of electron microscope images of thin crystals, the periodicities corresponding to the separations of prominent lattice planes of the crystals. The crystals concerned include metal phthalocyanines, (Menter, 1956*a*; Neider, 1956; Suito & Uyeda, 1957) faujasite (Menter, 1956*b*) and molybdenum trioxide (Bassett & Menter, 1957). The periodicities observed for these compounds corresponded to spacings of less than 20 Å and have been interpreted as given by interference of the first one or two diffracted beams with the transmitted beam, probably with changes of the relative phase of the interfering beams due to the spherical aberration of the objective lens.

On the other hand, several observations have recently been made of much larger periodicities, of the order of 100 Å, in which case it seems likely that the interference of the electron beams corresponding to at least the first few diffraction orders should not be seriously affected by lens aberrations. Examples include periodicities of about 40 and 90 Å observed in samples of antigorite by Brindley, Comer, Uyeda & Zussman (1958). Similarly, for the moiré-like fringes which appear in the electron microscope images of

superimposed crystals when there are slight differences in the size or orientation of the unit cell axes (see, for example, Mitsuishi, Nagasaki & Uyeda, 1951; Dowell, Farrant & Rees, 1954, 1956; Hashimoto & Uyeda, 1957; Bassett, Menter & Pashley, 1957; Goodman, 1957) when the periodicity is of the order of 100 Å or greater it can be expected that the image obtained with an electron microscope of high resolution is not greatly influenced by aberrations of the lenses and does not differ very much from the image which would be given by a perfect electron microscope except for details on a scale of 20 Å or less.

The question arises to what extent the periodicities observed in electron microscope images of crystals can be considered as images of the crystal lattice structure. Elementary considerations show that it is not sufficient to regard the crystal lattice as an amplitude object so that a dark line on the image is interpreted as a line of high density. Such an interpretation could lead to serious errors in explaining the detailed distribution of intensity in many of the micrographs which have been obtained from antigorite specimens or in many of the moiré fringe patterns which have been observed. There is a need, therefore, for an adequate theoretical treatment of the electron microscope imaging of crystal lattices.

The existing theoretical descriptions of the formation of an electron microscope image, such as those of Uyeda (1955) and Haine (1957), are concerned principally with the imaging of non-periodic objects and do not treat the question of imaging a crystal lattice specifically. Although their methods could undoubtedly be extended to include the case of crystal lattices, we prefer to base our discussion on the general theory of Cowley & Moodie (1958) and the theory of the scattering of electrons by crystals derived from it (Cowley & Moodie, 1957*a*, 1959), in which the necessary basic theoretical results have already been obtained.

A complete treatment of the formation of an electron microscope image could be divided into two parts: the modification of the incident electron wave by transmission through the specimen, and the modification of the resulting amplitude distribution by the magnifying lenses. In this paper we consider only the first of these two parts, and make the assumption that the lens system gives an image which is identical, apart from magnification, with the intensity distribution at the exit face of the crystal or in the object plane of the objective lens. Our results should thus correspond with observations of details in the image which are on a larger scale than the limit of resolution of the microscope, and so should be directly comparable with observations of the fringes of antigorite and moiré patterns. The results would have to be modified to take account of lens aberrations in order to give more than a very approximate account of the imaging of periodicities of about 20 Å or less.

2. Very thin crystals

When electrons pass through a crystal lattice, the relative phases of the different parts of the wave front are modified by the non-uniform potential field, giving rise to elastic scattering and interference effects. Inelastic scattering of the electrons gives rise to a decrease in the number of electrons transmitted without energy loss and also produces a distribution of inelastically scattered electrons which have appreciable energy losses. The contribution of the inelastically scattered electrons to the image depends on the chromatic aberrations of the electron lenses and the disposition and size of the apertures used. For simplicity we ignore this contribution, which has been stated to be relatively small (e.g., Haine, 1957), and consider only elastically scattered electrons.

In an earlier publication (Cowley & Moodie, 1957*a*) we showed that the effect of a potential field, $\varphi(x, y, z)$, of very small extent in the direction of the electron beam, the z-direction, is given by multiplying the wave function $\psi_0(x, y)$ representing the incident wave by

$$q_1(x, y) = \exp\{i\sigma\varphi(x, y) - \varrho\chi(x, y)\}, \qquad (1)$$

where

$$\varphi(x, y) = \int_{-\infty}^{\infty} \varphi(x, y, z)dz,$$

σ is a constant equal to $2\pi m\lambda/h^2$, $\chi(x, y)$ is a function analogous to $\varphi(x, y)$ for inelastic scattering and ϱ is the appropriate constant. Thus a thin crystal may be regarded as a combination of a phase grating and an amplitude grating. The intensity distribution at the exit face will be given by

$$\psi(x, y).\psi^*(x, y) = q_1(x, y).q_1^*(x, y) = \exp\{-2\varrho\chi(x, y)\}.$$

Thus the contrast in the in-focus image of the lattice produced by an ideal electron microscope is due entirely to the amplitude grating effect arising from inelastic scattering. Since the inelastic scattering term of (1) is very much less than the elastic scattering term, $\sigma\varphi(x, y)$, the in-focus contrast will be small for thin crystals; much less than that of a 'phase contrast' image.

It is well known that some contrast appears when a phase object is defocused. The nature of the out-of-focus images of periodic phases objects is discussed in detail in another publication (Cowley & Moodie, in preparation) in which expressions are derived for the intensity distributions of in-focus and out-of-focus Fourier images (Cowley & Moodie, 1957*b*, *c*, *d*) for objects periodic in one and two dimensions. It is sufficient to quote here some of the results for the one-dimensional case.

We assume that a plane wave is incident on a phase grating, the effect of which on the wave is given by multiplying by $q_1(x) = \exp\{i\sigma\varphi(x)\}$, where $\varphi(x) = \Sigma_h E_h \cos 2\pi hx/a$ has periodicity, a.

The deviation from focus is measured by a parameter given by $v = R\lambda/2a^2$, where R is the distance of the plane of observation from the grating. Then $v = \frac{1}{2}$ corresponds to the plane of the first Fourier image, which is an exact reproduction of the object so that the contrast in the image at this plane is zero.

If $v = \frac{1}{4}$ the intensity distribution is given by

$$I_{\frac{1}{4}}(x) = 1+\sin 2\sigma\varphi_0(x) ,$$

where

$$\varphi_0(x) = \sum_{h \text{ odd}} E_h \cos 2\pi hx/a ,$$

i.e., $\varphi_0(x)$ is obtained by putting all the even-numbered Fourier coefficients of $\varphi(x)$ equal to zero.

If v is very small, the intensity distribution is given by

$$I_v(x) = 1+\frac{a^2 v}{\pi}\frac{d^2\varphi(x)}{dx^2} .$$

Other values of v give more complicated expressions for the intensity.

It thus appears that, while the contrast due to elastic scattering from a crystal may be large when the electron microscope is defocused, the image produced is not a direct representation of the projected potential distribution, $\varphi(x, y)$, but may be calculated from the potential distribution if the defect of focus is known. Most of the electron micrographs showing the periodicity of a crystal lattice have been taken out of focus in order to increase the contrast of the fringes. Since the defect of focus is usually unknown it is not possible to relate the observed image to the crystal structures.

3. Thick crystals: the two-beam case

For crystal thicknesses in excess of a few hundred Å, the approximations of paragraph 2 above are no longer valid. The higher approximations described in an earlier paper (Cowley & Moodie, 1957*a*) may be applied for limited thickness ranges. One immediate result is that approximations beyond the first-order introduce amplitude as well as phase modulation due to pure elastic scattering.

No general solution to the problem of scattering from an arbitrarily thick crystal has yet been obtained, except in principle. We therefore make the usual assumption that there are only two strong beams in the crystal, the incident and one diffracted beam. This is sometimes a good approximation for thick perfect crystals, suitably oriented. Cowley & Moodie (1957*a*) derived the expression for the amplitude of the diffracted beam for this case, in the form

$$U_h = iF_h\,((\sin wH)/w)\,\exp\{i\sigma HE_0-\varrho HG_0-\pi i\zeta_h H\} , \quad (2)$$

where $w = (\pi^2\zeta_h^2+F_hF_{\bar{h}})^{\frac{1}{2}}$, F_h being the complex structure factor given by $F_h = \sigma E_h+i\varrho G_h$, ζ_h is the excitation error, or the distance in the beam direction of the Ewald sphere from the reciprocal lattice point denoted by h and H is the crystal thickness.

Starting from the same general equation and considering only contributions to the amplitude in the incident beam direction it is possible to derive in the same way the expression for the primary beam as

$$U_0 = [\cos wH-i(\pi\zeta_h/w)\sin wH] \times\exp\{i\sigma HE_0-\varrho HG_0+\pi i\zeta_h H\} . \quad (3)$$

The intensity distribution at the exit face of the crystal is then given by

$$\begin{aligned}\psi\psi^* &= |U_0+U_h\exp\{-2\pi ihx/a\}|^2\\ &= 1-\frac{2\sin wH}{w}\left\{\varrho G_h\cos wH+\frac{\pi\zeta_h}{w}\sigma E_h\sin wH\right\}\\ &\quad\times\cos 2\pi\left(\frac{hx}{a}-\zeta_h H\right)\\ &\quad-\frac{2\sin wH}{w}\left\{\sigma E_h\cos wH-\frac{\pi\zeta_h}{w}\varrho G_h\sin wH\right\}\\ &\quad\times\sin 2\pi\left(\frac{hx}{a}-\zeta_h H\right)\\ &= 1-2|F_h|\frac{\sin wH}{w}\left(\cos^2 wH+\frac{\pi^2\zeta_h^2}{w^2}\sin^2 wH\right)^{\frac{1}{2}}\\ &\quad\times\cos 2\pi\left(\frac{hx}{a}-\zeta_h H-\alpha\right) , \end{aligned} \quad (4)$$

where

$$2\pi\alpha = \tan^{-1}\left\{\frac{\sigma E_h\cos wH-(\pi\zeta_h/w)\varrho G_h\sin wH}{\varrho G_h\cos wH+(\pi\zeta_h/w)\sigma E_h\sin wH}\right\} ,$$

The image therefore consists of a set of cosine fringes for which both the amplitude of modulation, or contrast, and the phase depend in a complicated way on the modulus of the structure factor, $|F_h|$, the excitation error, ζ_h, and the crystal thickness, H.

When the crystal is set exactly at the Bragg angle, i.e., $\zeta_h = 0$, equation (4) reduces to

$$\psi\psi^* = 1-\sin 2|F_h|H\,.\cos 2\pi\left(\frac{hx}{a}-\alpha\right) . \quad (5)$$

where $2\pi\alpha = \tan^{-1}(\sigma E_h)/(\varrho G_h)$. (Since $\varrho G_h \ll \sigma E_h$, α is nearly equal to $\pi/2$). The contrast of the fringes therefore varies with the crystal thickness. If the crystal thickness varies, the intensity modulation goes to zero and changes sign for $2|F_h|H = n\pi$, n being an integer. The image of a wedge-shaped crystal giving a strong reflection from planes parallel to the plane of the wedge angle, would have the appearance indicated in Fig. 1, with a shift of $a/2$ in the fringes at each position of zero contrast. If the Bragg condition is not exactly satisfied, i.e., $\zeta_h \neq 0$, the appearance of the fringes will be similar but with different intervals between the positions of zero contrast.

To illustrate the dependence on excitation error, the contrast and phase of the fringes given by (4) are

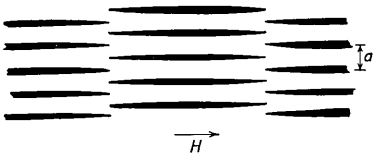

Fig. 1. The variation in intensity distributions of fringes corresponding to a crystal lattice spacing with varying crystal thickness, H.

plotted against excitation error for representative cases in Figs. 2(a) and (b). The values chosen are: $H = 200$ Å, $|F_h|H = \pi/3$ for Fig. 2(a) and $|F_h|H = \pi/2$ for Fig. 2(b).

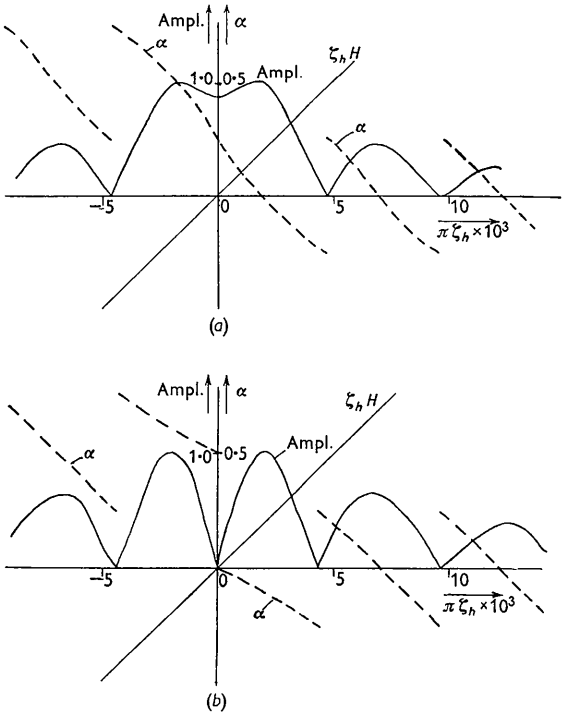

Fig. 2. The variation of contrast and phase angle of fringes given by a crystal of thickness 200π Å with $F_hH = \pi/3$ for 2(a) and $F_hH = \pi/2$ for 2(b), as a function of excitation error ζ.

For a crystal which is uniformly bent, so that ζ_h varies linearly with distance in the direction perpendicular to the axis of bending, Figs. 2(a) and (b) represent the distribution of contrast and phase of the fringes in the image. It is seen that the contrast decreases from the centre (the centre of the 'extinction contour' for a non-resolved lattice) through a series of maxima and zeros. At each position of zero contrast the phase jumps by π so that, unless the axis of bending is parallel to the reflecting plane, the fringe pattern will have the stepped structure of Fig. 1 with an apparent displacement of $a/2$ at each position of zero contrast.

The slopes of the curves for the phase angle α between discontinuities in Figs. 2(a) and (b) represent continuous phase changes which would have the effect of making the fringes in the image not quite parallel to the lattice planes. However the additional phase term ζ_hH in (4) has a similar but oppositely directed effect so that the fringes are in fact very nearly parallel to the lattice planes.

The effect of defocusing of the ideal electron microscope, which we assume is used to magnify the image formed at the exit face of the crystal, would be to add an additional constant phase factor in equation (4). This would displace all fringes by an equal amount and so would not effect the appearance of the image.

The case of dynamic scattering in a crystal of arbitrary thickness when two or more diffracted beams have appreciable intensity will not be treated here. From the calculations of Heidenreich (1950) and Hoerni (1956) it can be deduced that the periodicity of the modulation of the image will remain the same as that of the lattice, but the relative phases and amplitudes of the Fourier coefficients corresponding to the various diffracted beams will vary widely with crystal thickness and excitation error. The resulting image will in general have no recognizable relationship with the lattice structure.

Further, if the ideal electron microscope is defocused, the relative phases of the Fourier coefficients will be further changed since the phase shifts associated with defocusing depend on the spacing of the lattice planes concerned. An impression of the nature of this modification of the image can be obtained from the discussion of out-of-focus Fourier images by Cowley & Moodie (1957c).

4. Interpretation of electron micrograph observations on antigorite

Antigorite is a serpentine mineral having a superlattice unit cell with an a-axis usually of about 40 Å, i.e., about eight times the a-axis of the other serpentines. In an electron diffraction study of serpentine minerals, Zussman, Brindley & Comer (1957) found a-axes of 90 and 109 Å for a variety of antigorite known as Yu Yen Stone. Subsequently Brindley, Comer, Uyeda & Zussman (1958) reported the appearance of fringes corresponding to the 90 Å spacing in electron micrographs of lamellar crystals of this material. Uyeda, Masuda, Tochigi, Ito & Yotsumoto (1958) made further electron microscope observations and published several interesting micrographs. A similar micrograph, taken by Dr Ito, is reproduced in Fig. 3. In these the following features may be observed:

[1] The fringes vary in appearance, being sometimes sharp, sometimes broad, sometimes doubled and sometimes having weak subsidiary fringes.

[2] Dark bands with the appearance of extinction contours traverse the crystals. Near these the contrast of the fringes increases, and the fringe

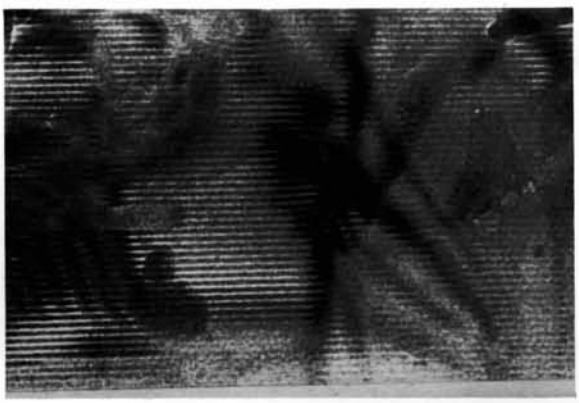

Fig. 3. Electron micrograph of an antigorite crystal showing the details of the behaviour of fringes due to the 90 Å superlattice reflection. (Taken by Dr K. Ito, and reproduced with his kind permission).

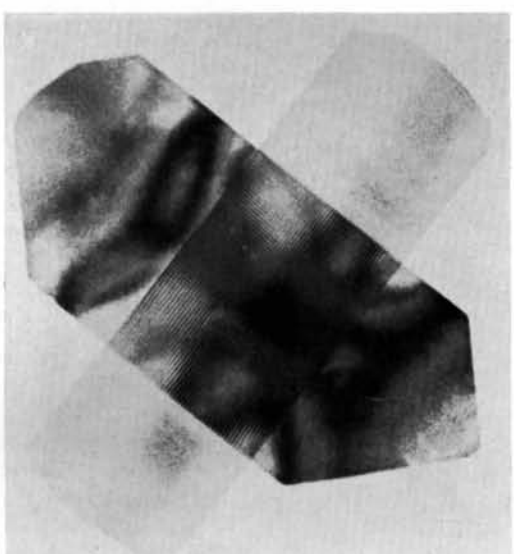

Fig. 6. Electron micrograph of crossed molybdenum oxide crystals showing the interaction of moiré-like fringes with extinction contours. (After Dowell, Farrant & Rees, 1954).

[*To face p.* 370

pattern has a 'stepped' appearance with an apparent phase difference of π between the fringes on either side of a band.

[3] The dark bands, and the associated stepped pattern have been observed to move relative to the crystal boundaries between observations.

[4] Other, more complicated effects are sometimes visible in limited regions of the crystal image.

These features, except for [3], can be seen in Fig. 3. If the appearance of the fringes is regarded as arising from dynamic scattering of the superlattice reflections, the varied appearance of the fringes as described in [1] may result from differences in thickness or in amount of defocus giving differences in the relative phases of the several dynamically scattered beams, as described at the end of section 3 above. Then localized changes in thickness by amounts of the order of $2|F_h|H$ would result in the stepped structures described in [2]. An explanation in these terms has been proposed by Hashimoto (private communication). This explanation would be satisfactory if evidence could be obtained that (*a*) the $|F_h|$ for the superlattice reflections are large enough to produce dynamic scattering in the observed crystal thicknesses, (*b*) local thickness variations of sufficient magnitude occur, and (*c*) the observation [3] above is illusory.

The value of $|F_h|$ for the strongest fundamental reflections for antigorite is probably such as to make $2|F_h|H = \pi$ for a value of H equal to several hundred Å. If this antigorite has a superlattice similar to that found by Kunze (1958), it seems highly probable that the structure factor for the superlattice reflections would be very much less than that of the fundamental reflections, so that thicknesses of thousands of Å would be required to produce dynamic effects.

An alternative explanation of the antigorite fringe observations is possible on the assumption that the superlattice reflections are kinematic, but that dynamic scattering of the fundamental reflections is taking place and giving rise to the extinction contours observed in the micrographs as dark bands.

We assume that a strong reflection, with structure factor F_g and excitation error ζ_g, occurs, but is intercepted by an aperture in the system and does not contribute to the image directly but modulates the primary beam, U_0, according to equation (3) with h replaced by g. The superlattice reflection U_h, with very small structure factor F_h and excitation error assumed to be very small, receives contributions from each part of the crystal proportional to the amplitude of the primary beam at that part. Thus the contribution to the superlattice reflection from a layer of thickness Δz at a distance z from the entrance face of the crystal is given by

$$U_h(z) = \exp(iHF_0).i\Delta z F_h \times [\cos wz - i(\pi\zeta_g/w)\sin wz]\exp\{\pi i\zeta_g z\},$$

where

$$w = (\pi^2\zeta_g^2 + F_g F_{\bar{g}})^{\frac{1}{2}}.$$

Then the total amplitude of the superlattice reflection is

$$U_h = \int_0^H U_h(z)\,dz = \exp(iHF_0)\frac{F_h}{F_g F_{\bar{g}}}\left[2\pi\zeta_g - \left\{2\pi\zeta_g\cos wH - \frac{i(w^2+\pi^2\zeta_g^2)}{w}\sin wH\right\}\exp\{\pi i\zeta_g H\}\right]. \quad (6)$$

If we consider the image to be formed by the primary beam and the superlattice reflections with indices h and $\bar{h}$, the intensity distribution on the image will be given by

$$\psi\psi^* = |U_0 + 2U_h\cos(2\pi hx/a)|^2 = 1 - (F_g^2/w^2)\sin^2 wH - \frac{4\pi\zeta_g\sigma E_h}{F_g F_{\bar{g}}}\left[\left(2 - \frac{F_g^2\sin^2 wH}{w^2}\right) - 2\left(\cos\pi\zeta_g H\cos wH + \frac{\pi\zeta_g}{w}\sin\pi\zeta_g H\sin wH\right)\right] \times \cos\frac{2\pi hx}{a}. \quad (7)$$

Here the inelastic scattering contribution σG_h has been ignored and terms of the second order of the quantity σE_h, assumed to be very small, have been omitted.

Equation (7) represents a set of cosine fringes for which both the contrast and background depend on the structure factor and excitation error of the fundamental reflection. For a bent crystal the position for which $\zeta_g = 0$ will be the centre of an extinction contour, which may take the form of a dark band or a set of dark bands. Since the contrast in the image given by (7) is an odd function of ζ_g there will be a change in sign of the contrast and hence a stepped structure with a displacement of the fringes by $a/2$ at the position $\zeta_g = 0$.

Intensity distributions have been calculated for two representative cases and are shown in Figs. 4(*a*) and (*b*), with contours of equal intensity plotted for variations in the coordinate x and the excitation error ζ_g, which is assumed to vary linearly perpendicular to the x coordinate as a result of a uniform bend in the crystal. The scale of ζ_g is such as to correspond to a bending about a very much smaller radius of curvature than would be encountered in practice. The diagrams should therefore be elongated horizontally by a very large factor for comparison with the electron micrograph observations. For Fig. 4(*a*), $H = 200\pi$ Å, $HF_h = 0{\cdot}15$ and $HF_g = \pi/2$, so that the intensity at the centre of the extinction contour is zero. For Fig. 4(*b*), $H = 200\pi$ Å, $HF_h = 0{\cdot}15$ and $HF_g = \pi$, so that the centre of the extinction contour has maximum intensity with a dark band on either side of it.

In each case the reversal of contrast, or stepped

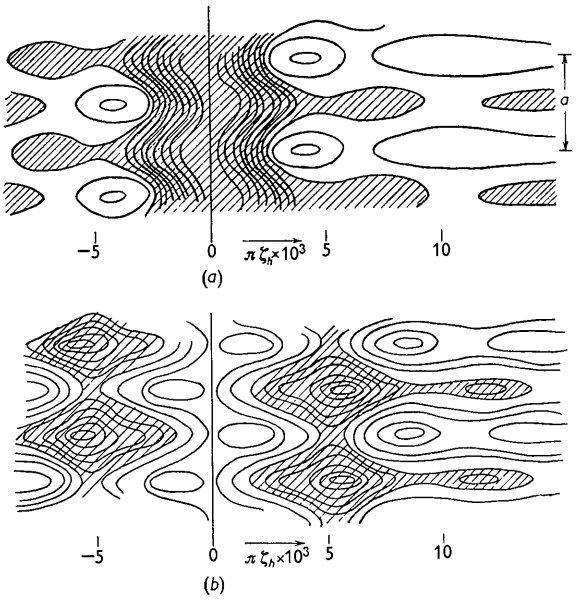

Fig. 4. Calculated intensity distributions for the antigorite superlattice fringes for a bent crystal, in the neighbourhood of an extinction contour due to dynamic scattering of a fundamental reflection. For 4(*a*), $F_gH = \pi/2$ and for 4(*b*) $F_gH = \pi$. Crystal thickness is $H = 200\pi$ Å.

appearance, can be seen about the $\zeta_g = 0$ position. The contrast of the fringes is greatest near the extinction contour, and decreases very slowly as ζ_g increases. It seems probable that in most cases the values of ζ_g for which the contrast becomes negligibly small will be greater than those required to make another neighbouring fundamental reflection operative. Hence the contrast of the fringes may be appreciable over large areas of the crystal even though the superlattice reflections are kinematic and would give no contrast in the absence of any fundamental reflections.

The principal features of the antigorite patterns have thus been satisfactorily explained. The motion of extinction contours and stepped structures between exposures, mentioned in item [3] above, can be explained in terms of slight changes in the bending or orientation of the crystals due to heating or electrostatic charging by the electron beam. Some of the more detailed features of the images of the fringes, such as the varied appearance of the fringes mentioned under [1], and the changes in appearance as fringes cross the extinction contours may also be explained if one takes into account the fact that most of the micrographs have been taken out of focus in order to increase the contrast.

According to Cowley & Moodie (1958, 1957*c*), the wave function in a plane at a distance R from the exit face of the crystal is given by

$$\psi_R(x) = \psi_0(x) * \exp\{-ikx^2/2R\}.$$

The off-focus distance may be expressed in terms of $\nu = R\lambda/2a^2$, as in section 2 above. Then the intensity distribution of the out-of-focus image is

$$\begin{aligned}\psi\psi^* = 1 &- \frac{F_g F_{\bar{g}}}{w^2}\sin^2 wH - \frac{4\pi\zeta_g\sigma E_h}{F_g F_{\bar{g}}}\cos\frac{2\pi hx}{a} \\ &\times\left[\left\{2 - \frac{F_g F_{\bar{g}}}{w^2}\sin^2 wH - 2\left(\cos wH.\cos\pi\zeta_g H\right.\right.\right. \\ &\left.\left. + \frac{\pi\zeta_g}{w}\sin wH.\sin\pi\zeta_g H\right)\right\}\cos 2\pi\nu h^2 \\ &+ \left\{\frac{F_g F_{\bar{g}}}{\pi\zeta_g w}\sin 2wH - 2\left(\cos wH.\sin\pi\zeta_g H\right.\right. \\ &\left.\left.\left. - \frac{\pi\zeta_g}{w}\sin wH.\cos\pi\zeta_g H\right)\right\}\sin 2\pi\nu h^2\right]. \qquad (8)\end{aligned}$$

It is readily verified that for $\nu = 0$, (8) reduces to (7). For $\nu = \frac{1}{4}$, which corresponds to maximum contrast in the kinematic case, the first term in the square bracket vanishes, and the contrast becomes an even function of ζ_g so that no phase reversal, or stepped appearance, occurs at the extinction contours. This is shown in the intensity plot of Fig. 5(*a*). However $\nu = \frac{1}{4}$ corresponds to a larger defocusing (about 8μ for a 90 Å spacing) than would normally be used. If, for example, we take $\nu = 0{\cdot}036$ so that $\cos 2\pi\nu = (9/2)\sin 2\pi\nu$, and consider the situation corresponding to Fig. 4(*a*), namely with $H = 200\pi$ Å, $HF_g = \pi/2$ and $HF_h = 0{\cdot}10$, the resultant intensity distribution is as shown in Fig. 5(*b*). The effect is that of adding

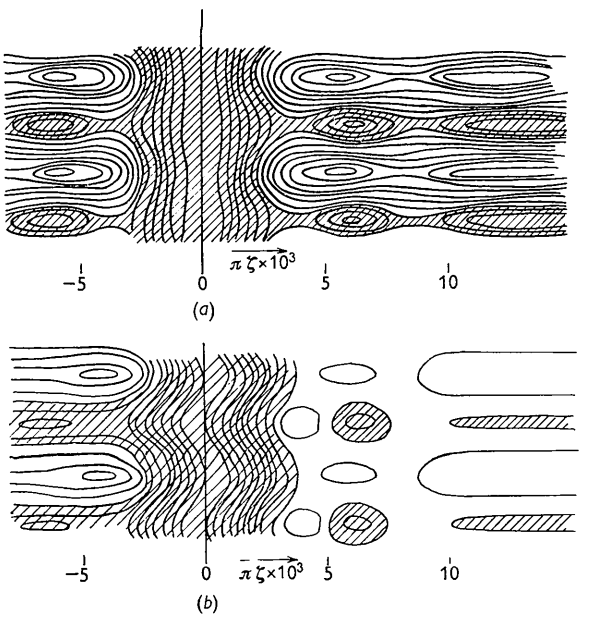

Fig. 5. Calculated out-of-focus intensity distributions corresponding to Fig. 4(*a*), with $\nu = \frac{1}{4}$ for 5(*a*) and $\nu = 0{\cdot}036$ for 5(*b*).

a fraction of the distribution of 5(*a*) to that of 4(*a*). The contrast of the fringes on the left-hand side has

been increased. On the right-hand side the contrast is at first decreased and then, with increasing ζ_g, is reversed. There is thus the appearance of a double phase reversal. Both the change in contrast across an extinction contour and the double-stepped appearance can be seen in several parts of Fig. 3.

A more complete account of some of the details of Fig. 3 can be given if we take into account the possibility that more than one pair of superlattice reflections contributes to the image. The equation (8) then takes the form

$$\psi\psi^* = 1-\frac{F_g F_{\bar{g}}}{w^2}\sin^2 wH - \frac{4\pi\zeta_g\sigma}{F_g F_{\bar{g}}}\sum_h E_h[\{\ldots\}\cos 2\pi\nu h^2 + \{\ldots\}\sin 2\pi\nu h^2]\cos\frac{2\pi hx}{a}.$$

There is thus, for each value of h, a set of fringes which may vary in form, from that of an even function, as in Fig. 5(*a*), to that of an odd function, as in Fig. 4(*a*), depending on the values of h, ν, H and F_g. Thus the Fourier coefficients of the fringe profile may vary in amplitude and phase from one side of the extinction contour to the other, giving differences in fringe appearance on the two sides, and there may be one, two, or no phase reversals. Fig. 3 contains examples of a number of the many possible combinations of predicted features.

In conclusion it may be stated that, in the presence of dynamic diffractions by lattice planes not contributing to the image, images may be produced by kinematic reflections which, by definition, are too weak to give appreciable contrast. The contrast of the fringes produced may vary widely, the fringes may appear sharp, diffuse or split into several components, and, at the extinction contours visible in images of bent crystals, the fringes may pass through one or more phase-reversing steps. It is to be expected that similar considerations will apply, with an even greater variety of possible results, if two-dimensionally periodic patterns of fringes are considered or if the possibility of dynamic scattering by the planes which are imaged is entertained. Considerable care must therefore be exercised in the interpretation of fringes appearing in the images of crystals in terms of crystal lattice structure.

5. Moiré-like patterns from thick crystals

The successive scattering of electrons by two thin crystals separated by an arbitrary distance has been treated in detail in another publication (Cowley & Moodie, to be published) on the assumption that the scattering is kinematic. It was shown that, when certain relationships are satisfied between the dimensions and orientations of the projected potential distributions $\varphi_1(x, y)$ and $\varphi_2(x, y)$ and the separation of the two crystals, it is possible to obtain a periodic modulation of the intensity of the image with a periodicity very much greater than that of either crystal lattice. The intensity distribution is then given by

$$\sum_h\sum_k E_1(h,k)E_2(-h,-k)\exp 2\pi i\left(\frac{hx}{A}+\frac{ky}{B}\right) = \varphi_1\left(\frac{x}{M},\frac{y}{M}\right) * \varphi_2\left(-\frac{x}{M},-\frac{y}{M}\right),$$

where A and B are the axes of the magnified unit cell and M is the magnification. If the two crystals are identical, this reduces to the Patterson function for the crystal projection.

The results obtained in section 3 above allow us to extend these results to the case where the scattering in the individual crystals is dynamic. Since we consider dynamic scattering for the two-beam case only, we deal with sets of parallel fringes with periodicity in one direction only and so can confine our treatment to one dimension.

In the relevant direction we consider the periodicities of the two crystals to be a_1 and a_2, the structure factors are E_1 and E_2 (ignoring inelastic scattering contributions), the excitation errors are ζ_1 and ζ_2 and the crystal thicknesses are H_1 and H_2.

The wave incident on the second crystal is that at the exit face of the first crystal, namely

$$\psi_1(x) = U_0' + U_h' \exp(2\pi i hx/a_1).$$

Applying our previous methods to calculate the scattering in the second crystal, it can be assumed that each term of the series which are summed to give U_0'' and U_h'' is therefore multiplied by $\psi_1(x)$ instead of $\psi_0(x) = 1$. At the exit face of the second crystal the intensity distribution is therefore given by

$$\psi\psi^* = |\{U_0' + U_h' \exp(2\pi i hx/a_1)\}\{U_0'' + U_{\bar{h}}'' \exp(-2\pi i hx/a_2)\}|^2. \quad (9)$$

The sign of h has been changed for the second crystal since we must assume a reflection opposite to that of the first crystal in order to get a diffracted beam close to the primary beam. Evaluation of (9) gives

$$\psi\psi^* = C_1^2C_2^2 + \sigma^4E_h^2E_{\bar{h}}^2\frac{\sin^2 w_1H_1}{w_1^2}\cdot\frac{\sin^2 w_2H_2}{w_2^2} - 2\sigma^2E_hE_{\bar{h}}C_1C_2\frac{\sin w_1H_1}{w_1}\cdot\frac{\sin w_2H_2}{w_2} \times\cos 2\pi\left(\frac{hx}{A}-\zeta_1H_1-\zeta_2H_2+\beta_1+\beta_2\right), \quad (10)$$

where

$$C_1 = \{\cos^2 w_1H_1 + (\pi^2\zeta_1^2/w_1^2)\sin^2 w_1H_1\}^{\frac{1}{2}}$$

and

$$2\pi\beta_1 = \tan^{-1}\left\{\frac{2\pi\zeta_1}{w_1}\tan w_1H_1\right\} = \frac{\pi}{2}-2\pi\alpha_1$$

and similarly for C_2 and β_2, and $(1/A) = (1/a_1)-(1/a_2)$,

A being the periodicity of the moiré-like fringes. In the derivation of (10), terms involving $\exp\{2\pi ix/a_1\}$ and $\exp\{2\pi ix/a_2\}$ have been omitted since these correspond to the unresolved spacings of the individual crystals.

Hence the background intensity, the contrast and the phase of the moiré-like fringes vary widely with the structure factors, crystal thicknesses and excitation errors for the two crystals. A clearer impression of the nature of the variations to be expected can be obtained by considering some special cases. For example, if the crystals can be assumed parallel we may take $\zeta_2 = -\zeta_1 = \zeta$. If one of the crystals, say the second, is very thin, we may take $\cos wH_2 = 1$, $\sin wH_2 \approx wH_2$. Then if we neglect terms in H_2^2 equation (10) reduces to

$$\psi\psi^* = C_1^2 - 2H_2\sigma^2 E_h E_{\bar{h}} C_1 \frac{\sin w_1 H_1}{w_1} \times \cos 2\pi\left(\frac{hx}{A} + 2\zeta H_1 + \beta_1\right). \quad (11)$$

This equation is similar to the equation (4) for a single dynamic crystal, $|F_h|$ being replaced by $H_2\sigma^2 E_h E_{\bar{h}}$, the constant background being replaced by C_1^2 which depends on ζ_1, F_h and H_1, and the phase angle α being replaced by $\beta_1 = \frac{1}{4} - \alpha$. The moiré-like fringes will therefore have much the same appearance as the fringes given by a single dynamically scattering crystal as described in section (3) above and illustrated in Fig. 2.

One noticeable difference between the two cases is that, whereas in equation (4) the phase contributions ζH and α very nearly cancelled out except for the discontinuities of π at the zero contrast positions, in equation (11) the contributions ζH_1 and β_1 modify the phase in the same direction as ζ changes. Because of the relatively large spacing of the moiré-like fringes it is possible that moderate bending of the crystal may introduce appreciable fringe displacements within distances comparable with the fringe periodicity. If the axis of bending is perpendicular to the fringes the phase variation will result in lateral displacement of the fringes giving them a slightly wavy appearance and changing their orientation with respect to the crystal lattices by small amounts. If the axis of bending is parallel to the fringes, the effect will be to make the spacing between the fringes vary.

These effects may be observed in Fig. 6 which is a reproduction of a micrograph published by Dowell, Farrant & Rees (1956) showing moiré-like fringes given by crossed crystals of molybdenum oxide. One of the crystals appears to be very thin since the extinction contours are very weak. The appearance and curvature of the extinction contours in the other crystal and in the common region indicates considerable bending. The three strong sets of moiré fringes, two parallel to the crystal edges and one diagonal, correspond to various pairs of strongly reflecting lattice planes. Careful inspection reveals that the fringes are appreciably deflected when crossed by extinction contours not parallel to them. The angle made by the fringes with the edges of the thinner crystal is also seen to vary.

A further interesting effect may be seen along the edges of the thicker (more heavily contoured) crystal. Near these edges the extinction contours, and hence the axis of bending, run parallel to the fringes. Hence one might expect an expansion or contraction of the fringe spacing. This effect, as can be seen from equations (10) and (11), should depend on the crystal thickness. Along the crystal edges there appears to be a very narrow strip of crystal of reduced thickness. Here it can be seen that the fringe spacing is reduced, giving the impression of one extra fringe per extinction band, and thus a false impression of the occurrence of edge dislocations at the crystal edges. Detailed calculations relative to this case have not been made in the absence of data on crystal thickness or curvatures. Approximate calculations however indicate that effects of the observed magnitude are predicted by equation (11). For example, a phase shift of 2π, or the displacement of fringes by a distance equal to the fringe spacing, takes place when the orientation of the lattice changes by 0·005 radians if the crystal thickness is 500 Å and the d-spacing of the contributing planes is 5 Å. There is therefore one extra or one less fringe in a distance of $0{\cdot}1\mu$ for a radius of curvature of 20μ.

From these limited considerations it is evident that, as in the case of the imaging of the lattices of individual crystals, extreme care is required in the interpretation of the appearance of the moiré-like fringes produced by overlapping crystals, especially if there is any evidence of dynamic scattering, such as the occurrence of extinction contours, or if the electron microscope is not focused exactly on the exit face of the crystals. Dynamic scattering effects may introduce displacements or distortions of the fringes, variations in contrast and in the intensity distributions across the fringes, stepped structures and changes in the fringe periodicity. Defect of focus may modify the pattern of fringes further and it is to be expected that the effect of lens defects, which has not been considered here, would be to add further complications.

I would like to express my sincere thanks to Dr K. Ito of the Japan Electron Optics Laboratory Co. Ltd., and Mr W. C. T. Dowell, Mr J. L. Farrant and Dr A. L. G. Rees of the Chemical Physics Division, C.S.I.R.O., for providing copies of their electron micrographs and for permission to reproduce them, and to Prof. R. Uyeda and Prof. H. Hashimoto for helpful discussions on the subject of the antigorite fringes.

References

BASSETT, G. A. & MENTER, J. W. (1957). *Phil. Mag.* **2**, 1482.

BASSETT, G. A., MENTER, J. W. & PASHLEY, D. W. (1957). *Nature, Lond.* **179**, 752.
BRINDLEY, G. W., COMER, J. J., UYEDA, R. & ZUSSMAN, J. (1958). *Acta Cryst.* **11**, 99.
COWLEY, J. M. & MOODIE, A. F. (1957*a*). *Acta Cryst.* **10**, 609.
COWLEY, J. M. & MOODIE, A. F. (1957*b*). *Proc. Phys. Soc.* B, **70**, 486.
COWLEY, J. M. & MOODIE, A. F. (1957*c*). *Proc. Phys. Soc.* B, **70**, 497.
COWLEY, J. M. & MOODIE, A. F. (1957*d*). *Proc. Phys. Soc.* B, **70**, 505.
COWLEY, J. M. & MOODIE, A. F. (1958). *Proc. Phys. Soc.* **71**, 533.
COWLEY, J. M. & MOODIE, A. F. (1959). *Acta Cryst.* **12**, 360.
DOWELL, W. C. T., FARRANT, J. L. & REES, A. L. G. (1954). Proceedings of the 3rd International Conference on Electron Microscopy, London, p. 279.
DOWELL, W. C. T., FARRANT, J. L. & REES, A. L. G. (1956). Proceedings of the Regional Conference on Electron Microscopy, Tokyo, p. 320.
GOODMAN, J. F. (1957). *Nature, Lond.* **180**, 425.
HAINE, M. E. (1957). *J. Sci. Instrum.* **34**, 9.
HASHIMOTO, H. & UYEDA, R. (1957). *Acta Cryst.* **10**, 143.
HEIDENREICH, R. D. (1950). *Phys. Rev.* **77**, 271.
HOERNI, J. (1956). *Phys. Rev.* **102**, 1534.
KUNZE, G. (1958). *Z. Kristallogr.*, **110**, 282.
MENTER, J. W. (1956*a*). *Proc. Roy. Soc.* A, **236**, 119.
MENTER, J. W. (1956*b*). Electron Microscopy, Proceedings of the Stockholm Conference, p. 88.
MITSUISHI, T., NAGASAKI, H. & UYEDA, R. (1951). *Proc. Japan Acad.* **27**, 86.
NEIDER, R. (1956). Electron Microscopy, Proceedings of the Stockholm Conference, p. 93.
SUITO, E. & UYEDA, N. (1957). *Proc. Japan Acad.* **33**, 398.
UYEDA, R. (1955). *J. Phys. Soc. Japan*, **10**, 256.
UYEDA, R., MASUDA, T., TOCHIGI, H., ITO, K. & YOTSUMOTO, H. (1958). *J. Phys. Soc. Japan*, **13**, 461.
ZUSSMAN, J., BRINDLEY, G. W. & COMER, J. J. (1957). *Amer. Mineral.* **42**, 133.

Acta Cryst. (1959). **12**, 375

Equi-Inclination Weissenberg Intensity Correction Factors for Absorption in Spheres and Cylinders, and for Crystal Monochromatized Radiation

BY W. L. BOND

Bell Telephone Laboratories, Inc., Murray Hill, New Jersey, U.S.A.

(*Received* 3 *March* 1958 *and in revised form* 8 *October and* 21 *November* 1958)

Increased precision of intensity measurements through the use of counting methods calls for more careful corrections. A new absorption correction table is presented for cylinders with μR running from 0 to 8 by tenths and on to 20 by units; also a table for spheres, μR running from 0 to 10 by tenths. In both tables θ runs from 0° to 90° in 5° steps. For cylinders, the correction factor for upper levels is gotten by entering the table with $\mu R \sec \nu$ in place of μR and $\Upsilon/2$ in place of θ, then multiply this value by $\cos \nu$. Tables are also given of the power series coefficients to be used in expanding absorption factors for very large cylinders. A combined polarization Lorentz correction factor is presented for the case of crystal monochromatized radiation.

Introduction

In recent years, there has been increasing emphasis on obtaining highly accurate structure amplitudes from single crystal X-ray data. In the course of work in these Laboratories on a single crystal automatic diffractometer (Bond, 1955; Benedict, 1955), several problems arose with regard to the conversion of intensities to structure amplitudes. These involved: (1) A Lorentz-polarization correction for monochromatized radiation; (2) expanding and improving the absorption tables for cylindrical and spherical crystals; and (3) deriving the method for absorption correction of upper level equi-inclination Weissenberg intensities. In particular, the latter has, as far as can be ascertained, been ignored. It is rather difficult to see how even for very small crystals containing light atoms, one can claim great accuracy (some claims have been 3%) for F's obtained say from layers with $\nu \cong 30°$ when such proper correction has not been made. As an example for $\mu R = 1$, $\mu = 20°$, $\Upsilon = 10°$ the absorption correction is 5·09 not 4·80 as is gotten from $\mu R = 1$, true $\theta = 20{\cdot}6°$.

Absorption correction tables

Consider scattering from a very small element of volume ΔV bathed in a uniform monochromatic collimated beam of X-rays. Let the beam be of intensity I watts cm.$^{-2}$ and let the scattering power in a direction parallel to a vector $\mathbf{r}$ be ϱ_r watts per cm.^{3}